Journal of ELECTRONIC MATERIALS, Vol. 44, No. 6, 2015
DOI: 10.1007/s11664-014-3435-4

Solid-State Synthesis and Thermoelectric Properties of $Mg_2Si_{0.5}Ge_{0.5}Sb_m$

SIN-WOOK YOU,[1] DONG-KIL SHIN,[1] SOON-CHUL UR,[1] and IL-HO KIM[1,2]

1.—Department of Materials Science and Engineering, Korea National University of Transportation, 50 Daehangno, Chungju, Chungbuk 380-702, Korea. 2.—e-mail: ihkim@ut.ac.kr

$Mg_2Si_{0.5}Ge_{0.5}Sb_m$ (m = 0, 0.005, 0.01, 0.02, and 0.03) solid solutions were synthesized by a solid-state reaction and consolidated by hot pressing. All specimens showed n-type conduction, and carrier concentrations were increased from 4.0×10^{17} cm^{-3} to 3.2×10^{21} cm^{-3} by Sb doping. The electrical conductivity remarkably increased with increasing Sb doping content, but the absolute value of the Seebeck coefficient was reduced as the Sb doping content increased, which was attributed to the increased carrier concentration. The lowest thermal conductivity was 2.3 W/mK for $Mg_2Si_{0.5}Ge_{0.5}Sb_{0.02}$ at 723 K, and the maximum ZT value of 0.56 was obtained for $Mg_2Si_{0.5}Ge_{0.5}Sb_{0.02}$ at 823 K.

Key words: Thermoelectric, magnesium silicide, solid solution, solid-state reaction

INTRODUCTION

Mg_2B^{IV} (B^{IV} = Si, Ge, Sn) and its solid solutions have attracted increasing attention as promising thermoelectric materials at temperatures ranging from 500 K to 800 K because they are non-toxic, environmentally friendly, and abundantly available.[1–4] The material factor $\beta = (m^*/m_e)^{3/2}\,\mu\kappa_L^{-1}$ can be utilized as the criterion for thermoelectric material selection, where m^* is the density-of-states effective mass, m_e is the mass of electron, μ is the carrier mobility, and κ_L is the lattice thermal conductivity. Consequently, thermoelectric materials with high performance should have a low lattice thermal conductivity and a high carrier mobility. The β for magnesium compounds Mg_2B^{IV} is 3.7–14, which is very high compared with 0.05–0.8 for iron silicides and 1.2–2.6 for silicon–germanium alloys.[5–11]

Among the solid solutions in the Mg_2B^{IV} systems, $Mg_2Si_{1-x}Ge_x$ has been known as one of the candidate thermoelectric materials since the late 1970s,[12] as it is stable at a composition of x = 0–1 and the thermal conductivity reaches the minimum when x is around 0.5. Song et al.[12] showed ZT = 0.2 at 610 K for $Mg_2Si_{0.6}Ge_{0.4}$ prepared by bulk mechanical alloying and hot pressing. Noda et al.[13] reported ZT = 0.68 at 629 K for Ag-doped $Mg_2Si_{0.6}Ge_{0.4}$. In this study, Sb-doped $Mg_2Si_{0.5}Ge_{0.5}$ solid solutions were synthesized by solid-state reaction and hot pressing. The electronic transport properties (Hall coefficient, carrier concentration and mobility) and thermoelectric properties (Seebeck coefficient, electrical conductivity, thermal conductivity and dimensionless figure of merit) were examined.

EXPERIMENTAL

$Mg_2Si_{0.5}Ge_{0.5}Sb_m$ (m = 0, 0.005, 0.01, 0.02, and 0.03) solid solutions were synthesized by a solid-state reaction (SSR) and hot pressing (HP). High purity Mg (99.99%, $<$149 μm), Si (99.99%, $<$45 μm), Ge (99.99%, $<$45 μm), and Sb (99.999%, $<$75 μm) powders were weighed as a stoichiometric ratio and mixed homogeneously. The mixed powders were cold-pressed under a pressure of 600 MPa to make pellets, which were reacted (transformed) in a solid state in a covered alumina crucible at 773 K for 6 h in a vacuum. The synthesized powders were hot-pressed in a cylindrical graphite die with an internal diameter of 10 mm at 1073 K under a pressure of 70 MPa for 2 h in a vacuum.

(Received April 29, 2014; accepted September 20, 2014; published online October 10, 2014)

The phases of synthesized solid solutions were analyzed by using an x-ray diffractometer (XRD; Bruker D8 Advance) using Cu K_α radiation (40 kV, 30 mA). The diffraction patterns were measured in the θ–2θ mode (10°–90° 2θ) with a step size of 0.02°, a scan speed of 0.4 s/step, and a wave length of 0.15405 nm. The hot-pressed compact was cut into a rectangular shape with the dimensions of 3 mm × 3 mm × 9 mm for both the Seebeck coefficient and the electrical conductivity measurements, and cut into a disc shape with dimensions of 10 mm (diameter) × 1 mm (thickness) for the thermal conductivity and the Hall effect measurements. The Hall effect measurements were carried out in a constant magnetic field (1 T) and electric current (50 mA) using the van der Pauw method at room temperature. The Seebeck coefficient and the electrical conductivity were measured using the temperature differential method and the 4-probe method, respectively, with ZEM-3 (Ulvac-Riko) equipment in a helium atmosphere. The thermal conductivity was estimated from the thermal diffusivity, specific heat and density measurements using a laser flash TC-9000H (Ulvac-Riko) system in a vacuum.

RESULTS AND DISCUSSION

Figure 1 shows the x-ray diffraction patterns for solid-state synthesized $Mg_2Si_{0.5}Ge_{0.5}Sb_m$ solid solutions. All specimens were identified as phases with anti-fluorite structures. The patterns of solid solutions correspond to Mg_2Si (ICDD PDF# 00-035-0773) and Mg_2Ge (ICDD PDF# 01-086-1028), with all the peaks located between pure Mg_2Si and Mg_2Ge. $Mg_2Si_{0.5}Ge_{0.5}Sb_m$ solid solutions have been successfully prepared by SSR and HP, and secondary phases were not found.

Table I summarizes the sintered densities and the transport properties of $Mg_2Si_{0.5}Ge_{0.5}Sb_m$ at room temperature. Undoped and Sb-doped $Mg_2Si_{0.5}Ge_{0.5}$ specimens showed n-type conduction, which meant that the majority carriers were electrons. The carrier concentration increased from 7.3×10^{17} cm^{-3} to 2.3×10^{21} cm^{-3} with increasing Sb content (m); consequently, the Sb atoms (Group B^V) were solved at Si or Ge sites (Group B^{IV}). However, the carrier mobility was decreased by Sb doping, which was a typical behavior of semiconductors caused by ionized impurity scatterings. As shown in Table I, the increase in the electron concentration was predominant over the decrease in the mobility caused by Sb doping; as a result, the electrical conductivity increased.

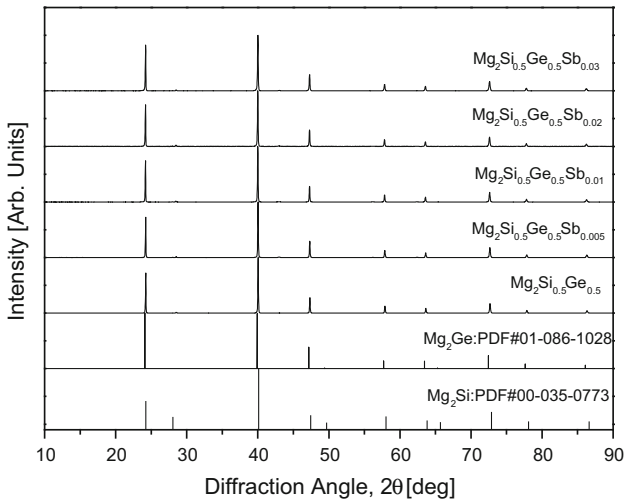

Fig. 1. X-ray diffraction patterns for $Mg_2Si_{0.5}Ge_{0.5}Sb_m$ solid solutions prepared by SSR-HP.

Figure 2 presents the temperature dependence of the electrical conductivity for $Mg_2Si_{0.5}Ge_{0.5}Sb_m$. The electrical conductivity (σ) of an n-type semiconductor is expressed as Eq. 1:

$$\sigma = \frac{ne^2\tau}{m^*} = ne\mu, \tag{1}$$

where e is the electronic charge, n is the electron concentration, μ is the electron mobility, m^* is the effective mass of electron, and τ is the relaxation time of the electron. The electrical conductivity of solid solutions increased from 3.3×10^2 S/m to 4.5×10^4 S/m by Sb doping, and was attributed to the increase in the carrier concentration. The electrical conductivity of the undoped specimen increased with increasing temperature, and behaved like a non-degenerate semiconductor. However, the Sb-doped specimens acted as degenerate semiconductors without temperature dependence.

Figure 3 shows the temperature dependence of the Seebeck coefficient for $Mg_2Si_{0.5}Ge_{0.5}Sb_m$. The Seebeck coefficient (α) of an n-type semiconductor is expressed as Eq. 2[14,15]:

$$\alpha = -\frac{k}{e}\left(\frac{5}{2} + r - \frac{E_C - E_F}{kT}\right) = -\frac{k}{e}\left(\frac{5}{2} + r + \ln\frac{N_C}{n}\right) \sim \gamma - c\ln n \tag{2}$$

where k is the Boltzmann constant, r is the exponent of the power function in the energy-dependent relaxation time expression, E_C is the bottom of the conduction band, E_F is the Fermi energy, T is the absolute temperature and N_C is the effective density-of-states in the conduction band, n is the charge carrier concentration, γ is the scattering factor, and c is a constant. Therefore, as shown in Fig. 3, the absolute value of the Seebeck coefficient ($|\alpha|$) of intrinsic $Mg_2Si_{0.5}Ge_{0.5}$ was very high at low temperature (−513 μV/K at 323 K), but it was reduced drastically with increasing temperature (−151 μV/K at 823 K) due to the increase in the electron concentration by intrinsic conduction.[16] The sign of the Seebeck coefficient was negative, which was in good agreement with the sign of the Hall coefficients shown in Table I. $|\alpha|$ was reduced

Table I. Relative densities and transport properties of $Mg_2Si_{0.5}Ge_{0.5}Sb_m$ at room temperature

Specimen	Relative density (%)	Hall coefficient ($cm^3\ C^{-1}$)	Mobility ($cm^2\ V^{-1}\ s^{-1}$)	Carrier concentration (cm^{-3})
$Mg_2Si_{0.5}Ge_{0.5}$	99.6	−8.44	28	7.3×10^{17}
$Mg_2Si_{0.5}Ge_{0.5}$:$Sb_{0.005}$	99.9	−0.044	4.2	1.4×10^{20}
$Mg_2Si_{0.5}Ge_{0.5}$:$Sb_{0.01}$	99.6	−0.004	0.9	1.5×10^{21}
$Mg_2Si_{0.5}Ge_{0.5}$:$Sb_{0.02}$	98.9	−0.003	0.88	2.0×10^{21}
$Mg_2Si_{0.5}Ge_{0.5}$:$Sb_{0.03}$	99.8	−0.0026	0.93	2.3×10^{21}

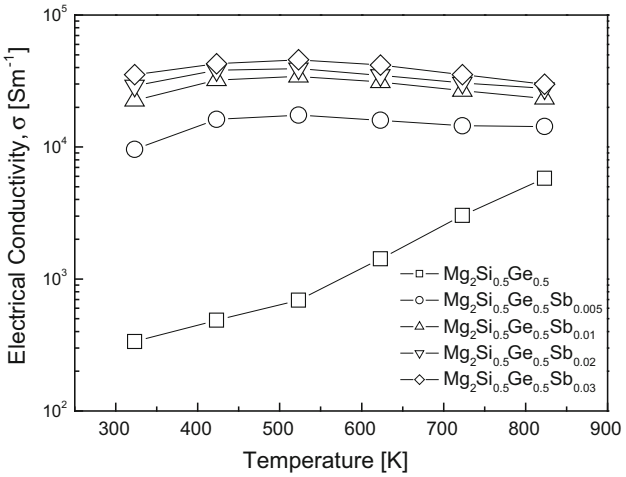

Fig. 2. Temperature dependence of the electrical conductivity for $Mg_2Si_{0.5}Ge_{0.5}Sb_m$.

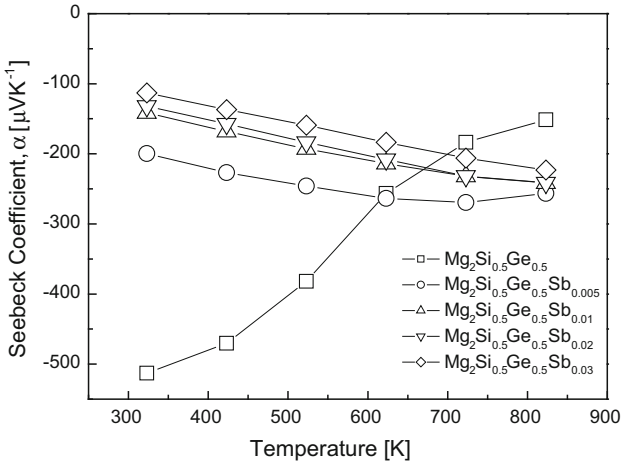

Fig. 3. Temperature dependence of the Seebeck coefficient for $Mg_2Si_{0.5}Ge_{0.5}Sb_m$.

as the Sb doping content increased, and this was attributed to the increased carrier concentration. $|\alpha|$ for Sb-doped $Mg_2Si_{0.5}Ge_{0.5}$ increased with increasing temperature, and decreased above a certain temperature. This resulted from the increase in the electron concentration by intrinsic conductions, and was predominant over the electron–phonon scattering at higher temperatures. The Seebeck coefficients of Sb-doped specimens ranged from −199 μV/K to −112 μV/K at 323 K, and from −256 μV/K to −222 μV/K at 823 K.

Figure 4 presents the temperature dependence of the thermal conductivity for $Mg_2Si_{0.5}Ge_{0.5}Sb_m$. The thermal conductivity (κ) is the sum of the lattice thermal conductivity (κ_L) by phonons and the electronic thermal conductivity (κ_E) by carriers. Both components can be separated by the Wiedemann–Franz law ($\kappa_E = L\sigma T$), where the Lorenz number was assumed to be a constant ($L = 2.45 \times 10^{-8}\ V^2\ K^{-2}$) for evaluation.[17] For all specimens, the thermal conductivity decreased with increasing temperature, and it increased by bipolar conduction caused by intrinsic excitation above 623 K for the undoped specimen and above 723 K for Sb-doped specimens. In the case of Sb-doped specimens, the intrinsic conduction temperature of Sb-doped specimens was higher than that of the undoped specimen. Sb doping slightly increased the thermal conductivity compared with intrinsic $Mg_2Si_{0.5}Ge_{0.5}$ due to higher electronic contribution, but it reduced the thermal conductivity above 723 K due to lower lattice contribution. The lowest thermal conductivity was 2.3 W/mK for $Mg_2Si_{0.5}Ge_{0.5}Sb_{0.02}$ at 723 K.

Figure 5 shows the temperature dependence of the dimensionless figure of merit (ZT) for $Mg_2Si_{0.5}Ge_{0.5}Sb_m$. As an index related to the energy conversion efficiency of thermoelectric materials, the ZT value was determined by Eq. 3[18]:

$$ZT = \frac{\alpha^2 \sigma T}{\kappa} \sim \left(\frac{m^*}{m_e}\right)^{3/2} \frac{\mu T^{5/2}}{\kappa_L}, \qquad (3)$$

where m_e is the mass of an electron. Therefore, a superior thermoelectric material should have a large Seebeck coefficient (large effective mass of carrier), high electrical conductivity (low carrier scattering), and low thermal conductivity (high phonon scattering), simultaneously.[15] The ZT values of an undoped specimen were very low, below 0.05, owing to low carrier concentration (low electrical conductivity). However, Sb doping significantly improved the electrical properties and maintained high values of the Seebeck coefficient and low thermal conductivity at high temperatures. Consequently, the ZT values remarkably increased, and the maximum ZT value of 0.56 was obtained for

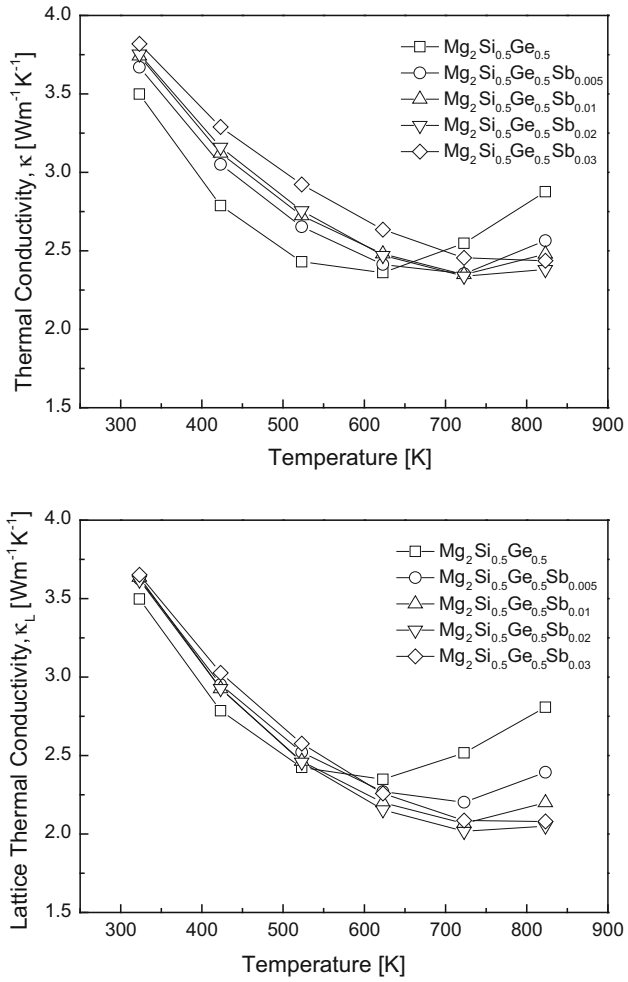

Fig. 4. Temperature dependence of the thermal conductivity for $Mg_2Si_{0.5}Ge_{0.5}Sb_m$.

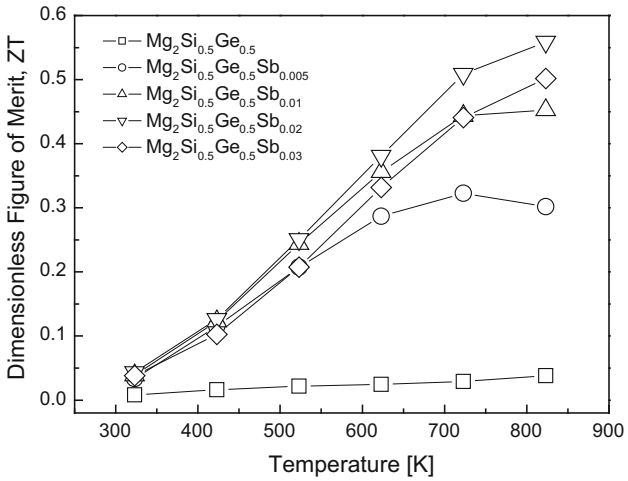

Fig. 5. Temperature dependence of the dimensionless figure of merit (ZT) for $Mg_2Si_{0.5}Ge_{0.5}Sb_m$.

$Mg_2Si_{0.5}Ge_{0.5}Sb_{0.02}$ at 823 K. Song et al.[12] and Aizawa et al.[19] reported $ZT = 0.2$ at 610 K and $ZT = 0.21$ at 613 K, respectively, for $Mg_2Si_{0.6}Ge_{0.4}$ prepared by bulk mechanical alloying and hot pressing. However, Zhou et al.[20] obtained very high ZT value of approximately 1.0 at 823 K for $La_{0.01}Mg_{1.99}Si_{0.49}Ge_{0.5}Sb_{0.01}$ prepared by spark plasma sintering. La/Sb co-doping was expected to control the carrier concentration and excess Mg was adopted to compensate for evaporative loss in their sample preparation.

CONCLUSIONS

Sb-doped Mg_2Si-Mg_2Ge solid solutions $Mg_2Si_{0.5}Ge_{0.5}Sb_m$ (m = 0, 0.005, 0.01, 0.02 and 0.03) were successfully prepared by a solid-state reaction and hot pressing. Sb-doped $Mg_2Si_{0.5}Ge_{0.5}$ showed n-type conduction. Carrier concentrations were increased from 4.0×10^{17} cm^{-3} to 3.2×10^{21} cm^{-3}, and the electrical conductivity was increased from 3.3×10^2 S/m to 4.5×10^4 S/m by Sb doping. The absolute value of the Seebeck coefficient was reduced as the Sb doping content increased; this was attributed to the increased carrier concentration. The Seebeck coefficients of Sb-doped $Mg_2Si_{0.5}Ge_{0.5}$ were from -256 μV/K to -222 μV/K at 823 K. The lowest thermal conductivity was 2.3 W/mK for $Mg_2Si_{0.5}Ge_{0.5}Sb_{0.02}$ at 723 K, and the maximum ZT value of 0.56 was obtained for $Mg_2Si_{0.5}Ge_{0.5}Sb_{0.02}$ at 823 K.

ACKNOWLEDGEMENT

This study was supported by the Regional Innovation Center (RIC) Program funded by the Ministry of Trade, Industry and Energy, Republic of Korea.

REFERENCES

1. Q. Zhang, J. He, T.J. Zhu, S.N. Zhang, X.B. Zhao, and T.M. Tritt, *Appl. Phys. Lett.* 93, 102109 (2008).
2. V.K. Zaitsev, M.I. Fedorov, E.A. Gurieva, I.S. Eremin, P.P. Kondtantinov, AYu Samunin, and M.V. Vedernikov, *Phys. Rev. B* 74, 045207 (2006).
3. J. Tani and H. Kido, *Phys. B* 364, 218 (2005).
4. W. Liu, X. Tang, H. Li, J. Sharp, X. Zhou, and C. Uher, *Chem. Mater.* 23, 5256 (2011).
5. W. Liu, Q. Zhang, X. Tang, H. Li, and J. Sharp, *J. Electron. Mater.* 40, 1062 (2011).
6. S. Bose, H.N. Acharya, and H.D. Banerjee, *J. Mater. Sci.* 28, 5461 (1993).
7. H.Y. Chen and N. Savvides, *J. Electron. Mater.* 38, 1056 (2009).
8. M. Akasaka, T. Iida, A. Matsumoto, K. Yamanaka, Y. Takanashi, T. Imai, and N. Hamada, *J. Appl. Phys.* 104, 013703 (2008).
9. H.L. Gao, X.X. Liu, T.J. Zhu, S.H. Yang, and X.B. Zhao, *J. Electron. Mater.* 40, 830 (2011).
10. V.K. Zaitsev, M.I. Fedorov, A.T. Burkov, E.A. Gurieva, I.S. Eremin, P.P. Kondtantinov, A.Y. Samunin, S. Sano, S.V. Ordin, and M.V. Vedernikov, *Proceedings of the 21st International Conference on Thermoelectrics,* Long Beach, CA, USA, 25–29 August (2002), p. 151.
11. K.H. Park, S.W. You, S.C. Ur, I.H. Kim, S.M. Choi, and W.S. Seo, *J. Korean Phys. Soc.* 60, 1485 (2012).
12. R. Song, Y. Liu, and T. Aizawa, *J. Mater. Sci. Technol.* 21, 618 (2005).
13. Y. Noda, H. Kon, Y. Furukawa, I.A. Nishida, and K. Masumoto, *Mater. Trans. JIM* 33, 851 (1992).
14. P.S. Kireev, *Semiconductor Physics* (Moscow: Mir Publishers, 1978), p. 253.

15. H.J. Goldsmid, *Electronic Refrigeration* (London: Pion Limited, 1985), p. 42.
16. S.W. You, K.H. Park, I.H. Kim, S.M. Choi, W.S. Seo, and S.U. Kim, *J. Electron. Mater.* 41, 1675 (2012).
17. C. Kittel, *Introduction to Solid State Physics*, 6th ed. (New York: Wiely, 1986), p. 152.
18. C.B. Vining, *Handbook of Thermoelectrics*, edited by D. M. Rowe (CRC Press, Boca Raton, 1995), p. 277.
19. T. Aizawa, R. Song, and A. Yamamoto, *Mater. Trans.* 46, 1490 (2005).
20. X. Zhou, G. Wang, H. Chi, X. Su, J.R. Salvador, W. Liu, X. Tang, and C. Uher, *J. Electron. Mater.* 41, 1589 (2012).